



**HAL**  
open science

## Non-Platinum metal oxide nano particles and nano clusters as oxygen reduction catalysts in fuel cells.

Louis Cindrella, Robert Jeyachandran

► **To cite this version:**

Louis Cindrella, Robert Jeyachandran. Non-Platinum metal oxide nano particles and nano clusters as oxygen reduction catalysts in fuel cells.. ENS 2007, Dec 2007, Paris, France. pp.101-106. hal-00202521

**HAL Id: hal-00202521**

**<https://hal.science/hal-00202521>**

Submitted on 7 Jan 2008

**HAL** is a multi-disciplinary open access archive for the deposit and dissemination of scientific research documents, whether they are published or not. The documents may come from teaching and research institutions in France or abroad, or from public or private research centers.

L'archive ouverte pluridisciplinaire **HAL**, est destinée au dépôt et à la diffusion de documents scientifiques de niveau recherche, publiés ou non, émanant des établissements d'enseignement et de recherche français ou étrangers, des laboratoires publics ou privés.

**NON-PLATINUM METAL OXIDE NANO PARTICLES AND NANO CLUSTERS AS OXYGEN REDUCTION CATALYSTS IN FUEL CELLS**

*L.Cindrella<sup>1</sup> and R.Jeyachandran<sup>2</sup>*

<sup>1</sup>Department of Chemistry, National Institute of Technology  
Tiruchirappalli 620015, India

<sup>2</sup>Department of Biotechnology, St.Joseph's College  
Tiruchirappalli 620002, India

**ABSTRACT**

An attempt has been made in this study to prepare the oxygen electrodes containing low-scale particles of copper, nickel, cobalt and iron oxides and evaluate their catalytic activity for the oxygen reduction. 1:1 stoichiometric oxides (Copper and Nickel) and higher stoichiometric oxides (Cobalt and Iron) have been synthesized and their catalytic properties have been analyzed by electrochemical methods. The conductivity of the fabricated electrodes showed steady values even with change in temperature from the ambient ( $30 \pm 2^{\circ}\text{C}$ ) to  $70^{\circ}\text{C}$ .

**1. INTRODUCTION**

The significance of porous carbon electrodes [1] for oxygen reduction in fuel cells [2] is well known. The use of platinum catalyst on carbon electrode to favour the kinetics of oxygen reduction is widely practiced [3]. Due to the higher cost of platinum and the necessity for other alternatives [4], recent research aims at the platinum equivalents, bimetallics and trimetallics [5]. As oxides [6] have shown good conductivity and the relative ease with which they could be obtained and handled, they offer themselves as the promising materials for electrochemical

energy applications. Hence the present research aims at the catalysts alternative to platinum with a thrust to make the fuel cells cost effective.

**2. EXPERIMENTAL**

In a low concentration bath with the continuous flow of the reagent under optimized conditions (Temperature– $30^{\circ}\text{C}$ ), the hydroxides of copper, nickel, cobalt and iron were prepared using the exact Stoichiometric ratio of the reagents. The precipitates were dried under vacuum at  $60^{\circ}\text{C}$  in a rotary evaporator and incinerated at the optimized temperature and the oxides obtained were characterized by X-Ray Diffraction (XRD) analysis. The XRD patterns of the systems studied are given in Fig.1 to Fig.4. The five most intense peaks are indexed and the data provided confirmation that the methodology that we have optimized, gives rise to reproducible products. The FTIR spectra of the samples were analysed in the range of  $4000 - 450\text{ cm}^{-1}$ . The electrode material was prepared by mixing intimately the activated charcoal (  $5 - 8\text{ }\mu\text{m}$  particle size), PTFE binder and the catalysts prepared, in the weight ratio, 89:10:1. The electrodes were prepared by compaction technique (load pressure  $125\text{ kg/cm}^2$ ). The conductivity of the electrodes were studied by four probe technique and the rest potential of the

electrodes and for reduction of oxygen were analyzed by potentiostatic technique.

### 3. RESULTS AND DISCUSSION

Our attempt to synthesize the oxides in different lattices could be achieved by the proper choice of the precursors. The XRD patterns of the systems studied are given in Fig.1 to Fig.4. The five most intense peaks are indexed and the data provided confirmation that the methodology that we have optimized gives rise to reproducible products.

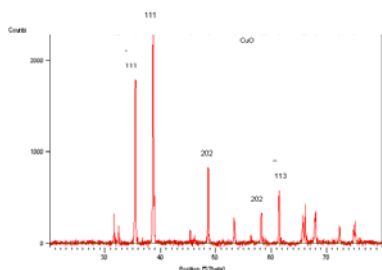


Fig.1. XRD pattern of copper oxide (Monoclinic System end-centered lattice, Cell parameters:  $a = 4.683$ ,  $b=3.422$ ,  $c=5.128$ ,  $\beta=99.54$ )

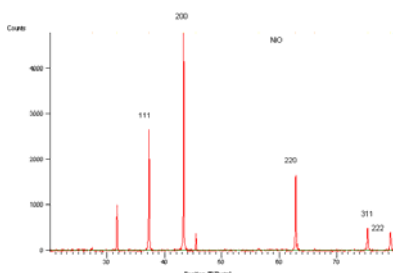


Fig.2. XRD pattern of nickel oxide (FCC system, Cell parameter:  $a = 4.180$ )

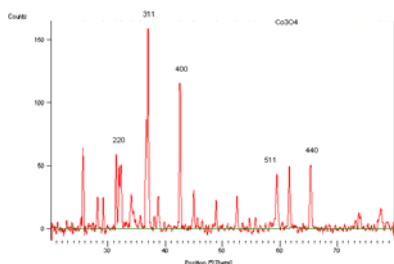


Fig.3. XRD pattern of cobalt oxide (FCC System, Cell parameters :  $a = 8.083$  )

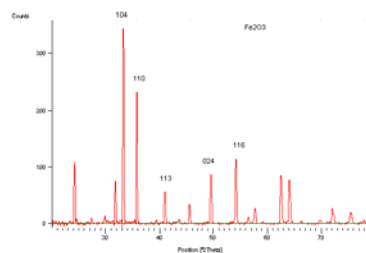


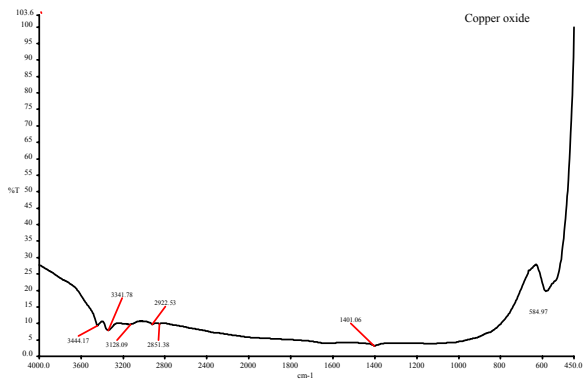
Fig.4. XRD pattern of iron oxide (Hexagonal system, Rhomb-centered lattice, Cell parameters:  $a = 5.014$ ,  $c = 13.67$ )

While the nickel oxide and cobalt oxide have been obtained in the FCC system, copper oxide has been obtained in the monoclinic system and the iron oxide in the hexagonal rhomb-centered lattice.

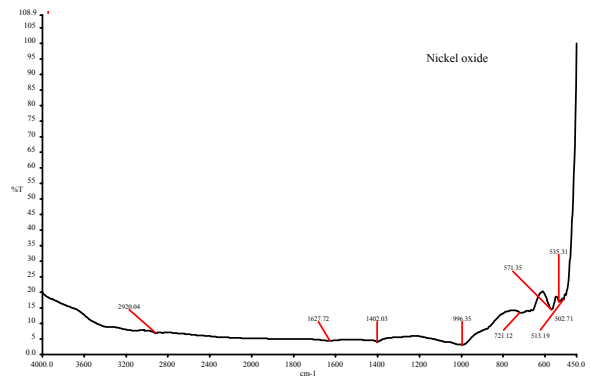
The FT IR spectra (Fig.5) of all the four samples showed the metal-oxygen stretching, whereas the  $-OH$  stretching,  $-OH$  bending, carbonate stretching frequencies were totally absent, inferring high purity of the sample obtained and without the formation any carbonate from the environmental  $CO_2$  and also the residual hydroxides.

Figures 6 to 9 reveal the SEM images of the particles prepared in this study. Fig.6 shows the uniform size distribution of iron oxide by about 160 nm. Fig. 7 exhibits the size distribution of nickel oxide in the range of 160 nm and as its multiple. The nickel oxide requires stabilization to avoid agglomeration. But the grain boundary of the individual particles could be easily traced. The SEM image of cobalt oxide (Fig.8) shows wider variation in the particle size between 260 nm and 1580 nm. The percentage of the low-scale particles is high. Fig.9. shows the SEM image of copper oxide, with size range of 500nm and above. The

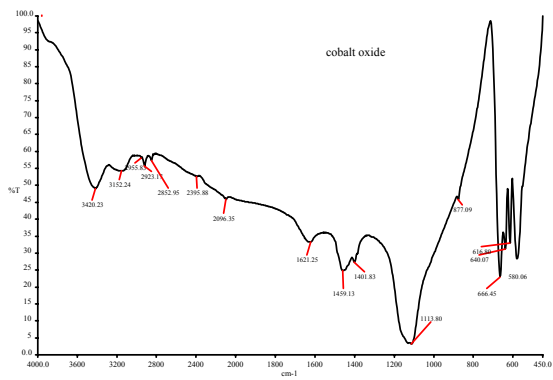
SEM reveals a uniform particle size of iron oxide, short



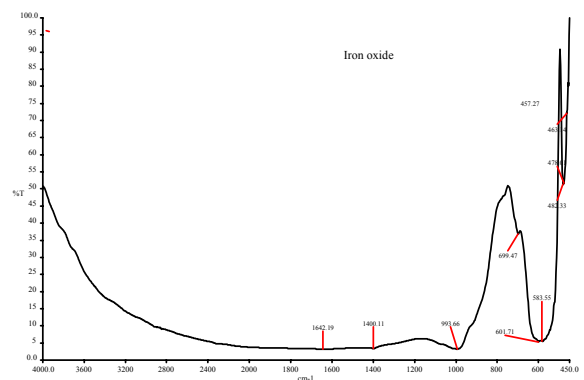
(a)  
FT IR spectra of copper oxide



(b)  
FT IR spectra of nickel oxide



(c)  
FT IR spectra of cobalt oxide



(d)  
FT IR spectra of iron oxide

Fig.5.

range of distribution of the particles in the case of nickel oxide highlighting the reproducible method of material preparation. In the other two cases, further optimization for nano scale particles is attempted by electrokinetic processes.

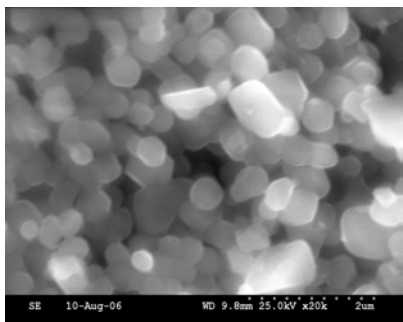


Fig. 6. SEM image of iron oxide

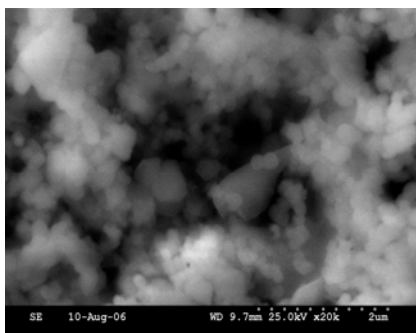


Fig. 7. SEM image of nickel oxide

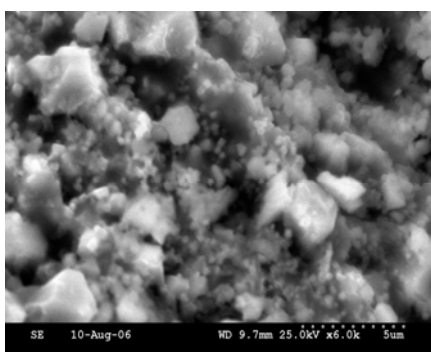


Fig.8. SEM image of Cobalt oxide

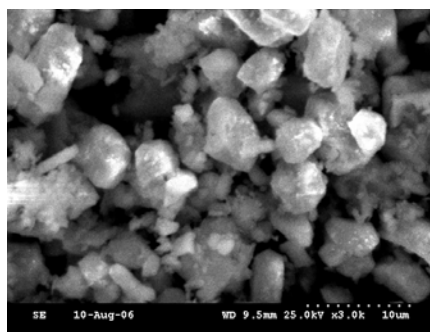


Fig.9. SEM image of Copper oxide

The Carbon electrodes of 1.3 cm diameter, prepared by compaction method by incorporating the catalysts are shown in Fig.10. The electrical resistivity of the electrodes as measured with a four-point probe method, revealed an average bulk electrical conductivity of the optimized electrodes as  $10 \text{ S cm}^{-1}$ . As the preparation, compaction and sintering steps influenced the bulk conductivity, scope for further improvement in the electrical conductivity by optimization is a promising route. The rest potentials (Vs Ag/AgCl) of the carbon electrode with and without the catalysts were measured in 4M KOH solution. The equilibrium potential of the catalyst-loaded electrodes recorded 100 mV higher than that of the carbon electrode without the catalysts.

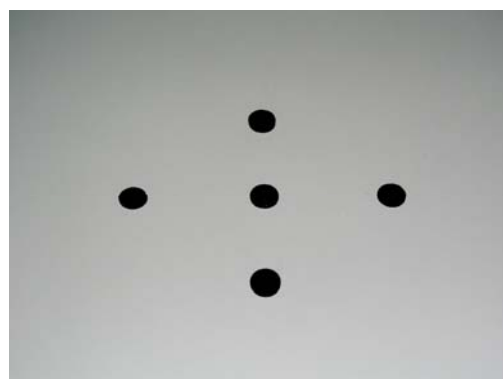


Fig.10. Carbon electrodes, fabricated with the catalysts by compaction.

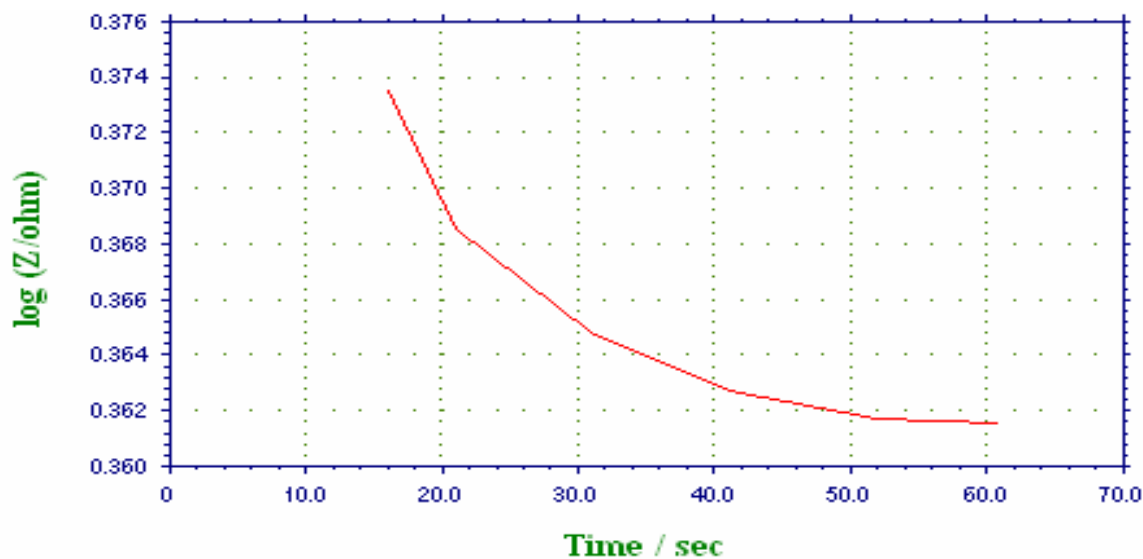


Fig.11. Log Z Vs time plot for the electrode systems.

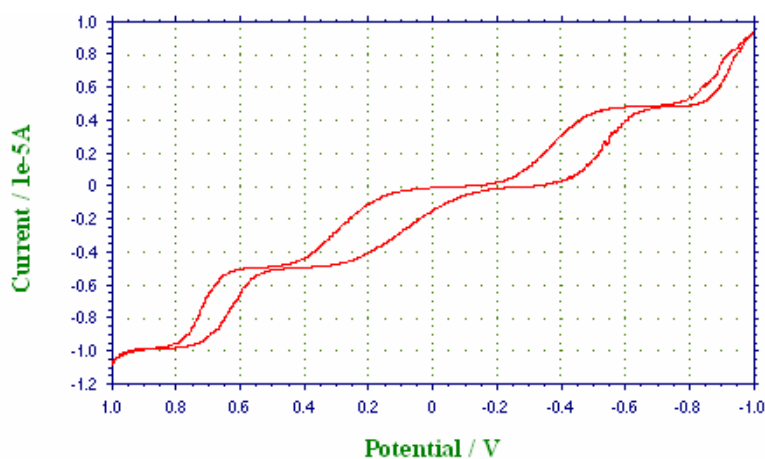


Fig.12. Cyclic voltammogram of oxygen reduction in alkaline medium using the metal oxide catalysts.

$R_{act}$  has been deduced from the AC impedance spectroscopy [7]. The Nyquist diagrams for all the fabricated electrodes Vs Ag/AgCl and in the Al-air and Zn-air fuel cells have been obtained. The drastic reduction in the activation polarisation due to the catalysts, especially in the cases of iron and nickel systems highlight the

particle size effect on the catalytic activity. The improved kinetics of the oxygen reduction as revealed by the AC impedance spectroscopy brings to light the usefulness of these catalysts for the oxygen reduction. The typical impedance plot for all the systems studied is shown in Fig.11.

The multi step reduction in alkaline medium is demonstrated in Fig.12.

Optimization of the system for selective reduction at a higher kinetics of otherwise sluggish reduction of oxygen is under progress.

#### 4. CONCLUSION

Metal oxide catalysts for oxygen reduction have been synthesized and characterized for their compositions and functions. Such cheap materials will pave way for the substitution or as supplement for the platinum based catalysts.

#### 5. REFERENCES

[1] H.A. Liebhafsky and E.J.Cairns, Fuel Cells and Fuel Batteries, John Wiley & Sons, NY, 1968.

[2] Mathias, M.F., J.Roth, J.Fleming and W.Lehnert, "Diffusion media materials and characterization, in W.Vielstich, A.Lamm, and H.A. Gastegier(ed), Handbook of Fuel Cells, Fundamentals, Technology and Applications, Vol.3 Fuel cell Technology and Applications, John Wiley & Sons, NY, pp.517-537, 2003.

[3] Ralph, T.R. and M.P. Hogarth, "Catalysis for low temperature fuel cells, Part I: the Cathode Challenges", Platinum Metals Review, Vol. 46, No.1, pp.3-14, 2002.

[4] V. Mancier, A.Metrot and P.Willmann, "AC impedance modeling of nickel hydroxide electrodes viewed as mixed protonic-electronic conductors". Electrochim.Acta, 41, p.1259, 1996.

[5] Zhen-Bo Wang, Ge-Ping Yin and Yong-Ge Lin, "Synthesis and characterization of PtRuMo/C nanoparticle

electrocatalyst for direct ethanol fuel cell", Journal of Power Sources, 170, pp.242-250, 2007.

[6] J.W.Kim and S.M.Park, "Electrochemical oxidation of ethanol at thermally prepared RuO<sub>2</sub>-Modified electrodes in alkaline media", J.Electrochem. Soc., 146, p.1075, 1999.

[7] S.M. Park and J.S.Yoo, "Electrochemical impedance spectroscopy for better electrochemical measurements", Anal.Chem. 75, 455A, 2003.